

# Hard X-ray-Induced Valence Tautomeric Interconversion in Cobalt-*o*-Dioxolene Complexes.

Thiago M. Francisco<sup>1</sup>, William J. Gee<sup>2</sup>, Helena J. Shepherd<sup>2</sup>, Mark R. Warren<sup>3</sup>, David A. Shultz<sup>4</sup>, Paul R. Raithby<sup>5</sup> and Carlos B. Pinheiro<sup>1\*</sup>.

1. Physics Department, Federal University of Minas Gerais, Belo Horizonte, 31270-901, Brazil
2. School of Physical Sciences, University of Kent, Canterbury CT2 7NZ, United Kingdom
3. Diamond Light Source, Ltd., Harwell Science & Innovation Campus, Didcot OX11 0DE, United Kingdom
4. Department of Chemistry, North Carolina State University, Raleigh, North Carolina 27695, United States
5. Department of Chemistry, University of Bath, Bath BA2 7AY, United Kingdom

\*E-mail: [cbpinheiro@ufmg.br](mailto:cbpinheiro@ufmg.br).

## Supporting Information

### X-ray experiment Description

The structure of  $[\text{Co}(\text{diox})_2(4\text{-CN-py})_2]\cdot\text{benzene}$  complex (**1**) (*diox* = 3,5-di-*t*-butylsemiquinonate, ( $\text{SQ}^\bullet$ ) and/or 3,5-di-*t*-butylcatecholate ( $\text{Cat}^{2-}$ ) radical; 4-CN-py = 4-cyano-pyridine) was probed at various temperatures using hard X-rays. Single crystal X-ray diffraction data were collected at I19 - the small-molecule single-crystal diffraction beamline at Diamond Light Source,<sup>1</sup> which has a flux of about  $10^{10}$  photons  $\text{s}^{-1}$ , distributed over spot of  $0.1 \times 0.1 \text{ mm}^2$  - using the 0.4859 Å radiation (25516.4 eV). A commercially available open-flow He cryostat apparatus (nHeliX, Oxford Cryosystems), with stability better than  $\pm 0.3 \text{ K}$ , was used to control the sample temperature. Two different single crystals samples (Sp1, Sp2) suitable for X-ray diffraction experiments were mounted in a capton loop and investigated. Two experiments were undertaken in order to qualitatively assess the effects of the hard X-rays on the samples.

In the so-called HAX experiment, the sample Sp1 was fast-cooled from 290 K down to 30 K, measured at 30 K, then measured at 30 K once more in a very long experiment for electron density investigation, and then successively measured using hard X-rays in a sequence shown in Table S1.

Table S1. Sequence of hard X-rays (HAX) experiments performed using sample Sp1. Temperature error  $\pm 2 \text{ K}$ .

Experiment Code	Time duration (min)	Temperature (K)	Data Resolution	Data Completeness	Data Redundancy
HAX1 <sup>(i)</sup>	22	30	0.71	0.594	8
HAX2 <sup>(ii)</sup>	301	30	0.44	0.907	16
HAX3	22	40	0.70	0.990	15
HAX4	21	50	0.71	0.990	15
HAX5	21	60	0.71	0.991	14
HAX6	22	70	0.70	0.992	14
HAX7	21	80	0.71	0.992	14
HAX8	21	90	0.71	0.992	14
HAX9	22	100	0.72	0.993	15

(i) Used for evaluation of the time dependence of the metastable  $\text{hs-}[\text{Co}^{+2}(\text{SQ}^\bullet)_2]$  isomer mole percentage growth; (ii) long high resolution data for electron density studies.

Experiments HAX1 and HAX2 were used to evaluate the time dependence of the metastable  $hs-[Co^{+2}(SQ^{\bullet})_2]$  isomer mole percentage growth. The duration of each run is indicated in Table S2.

Table S2. Time duration of the partial hard X-rays (HAX) runs performed using sample Sp1.  
Temperature error  $\pm 2$  K.

Experiment Code	Run	Time duration (min)	Temperature (K)	Data Resolution	Data Completeness	Data Redundancy
HAX1 <sup>(i)</sup>	1	5	30	0.71	0.822	2.7
	2	5	30	0.71	0.873	2.7
	3	5	30	0.71	0.800	3.0
	4	5	30	0.71	0.823	2.9
HAX2 <sup>(ii)</sup>	1	25	30	0.44	0.907	1.1
	2	25	30	0.44	0.908	1.0
	3	25	30	0.44	0.906	1.0
	4	25	30	0.44	0.916	1.2
	5	23	30	0.43	0.800	1.0
	6	22	30	0.44	0.886	1.0
	7	24	30	0.44	0.898	1.2
	8	25	30	0.44	0.594	1.2

(i) Used for evaluation of the time dependence of the metastable  $hs-[Co^{+2}(SQ^{\bullet})_2]$  isomer mole percentage growth; (ii) long high resolution data for electron density studies.

In a second experiment, the sample Sp2 was slowly cooled from 290 K down to 30 K. The sequence of successive measurements (AHAX) shown in Table S3 was performed under cooling using a 78% attenuated X-ray beam thanks to a 3mm thick aluminum filter. In the last experiment (AHAX13), attenuation filter was removed and a final experiment was made to evaluate the time dependence of the metastable  $hs-[Co^{+2}(SQ^{\bullet})_2]$  isomer mole fraction growth

Table S3. Sequence of attenuated hard X-rays (AHAX) experiments performed using sample Sp2.  
Temperature error  $\pm 2$  K.

Experiment Code	Time duration (min)	Temperature (K)	Data Resolution	Data Completeness	Data Redundancy
AHAX1	30	110	0.71	0.969	4.2
AHAX2	29	90	0.72	0.977	4.8
AHAX3	29	75	0.71	0.978	5.0
AHAX4	29	60	0.71	0.977	5.1
AHAX5	30	45	0.70	0.978	5.1
AHAX6 <sup>(i)</sup>	30	30	0.72	0.977	5.0
AHAX7 <sup>(ii)</sup>	30	30	0.70	0.979	5.1

(i) Used for evaluation of the time dependence of the metastable  $hs-[Co^{+2}(SQ^{\bullet})_2]$  isomer mole percentage growth; (ii) non attenuated beam data collection performed after AHAX data dataset.

Experiments AHAX6 and AHAX7 were used to evaluate the time dependence of the metastable  $hs-[Co^{+2}(SQ^{\bullet})_2]$  isomer mole percentage growth. The duration of each run of these experiments is indicated in Table S4.

Table S4. Time duration of the partial hard X-rays (AHAX) runs performed using sample Sp1.  
Temperature error  $\pm 2$  K.

Experiment Code	Run	Time duration (min)	Temperature (K)	Data Resolution	Data Completeness	Data Redundancy
AHAX6 <sup>(i)</sup>	1	22	30	0.71	0.915	1.2
	2	301	30	0.71	0.838	1.2
AHAX7 <sup>(ii)</sup>	1	22	30	0.71	0.919	1.6
	2	301	30	0.71	0.840	1.2

(i) Used for evaluation of the time dependence of the metastable  $hs-[Co^{+2}(SQ^{\bullet})_2]$  isomer mole percentage growth; (ii) non attenuated beam data collection performed after AHAX data dataset.

For each measured temperature, and/or individual partial runs, the X-ray diffraction data integration and scaling of the reflection intensities were performed with the *Crystall Suite*.<sup>2</sup> Final unit cell parameters were based on fitting of all measured reflection positions. Semi-empirical absorption corrections based on the intensities averaging was performed using *Crystall Suite*.<sup>2</sup> Structure was solved by direct methods using the *SIR92*<sup>3</sup> program and the positions of all non-hydrogen atoms of **1** were unambiguously assigned on consecutive difference Fourier maps. Refinements were performed using *SHELXL2016*<sup>4</sup> based on  $F^2$  through full-matrix least-squares routine. Hydrogen atoms were located in Fourier difference maps and included as fixed contributions according to the riding model<sup>5</sup> [C–H and N–H = 0.97 Å and  $U_{\text{iso}}(\text{H}) = 1.2 U_{\text{eq}}(\text{C or N})$  for methylene and aromatic groups and carbon atoms]. All non-hydrogen atoms of **1** were refined with anisotropic atomic displacement parameters. A summary of the crystal data, measurement and refinement data, for representative temperatures are shown in Tables S4–S6. CCDC<sup>6</sup> CIF files 1559584–1559598 contain the supplementary crystallographic data for this paper. They can be obtained free of charge from The Cambridge Crystallographic Data Centre via <https://www.ccdc.cam.ac.uk/structures/>.

Table S5. Crystal data, measurement and refinement data for representative hard X-rays (HAX) experiments.

Measurement Code	HAX1 (RUN1)*	HAX2 (RUN8) *	HAX2	HAX6
Empirical formula	CoC <sub>52</sub> H <sub>60</sub> N <sub>4</sub> O <sub>4</sub>	CoC <sub>52</sub> H <sub>60</sub> N <sub>4</sub> O <sub>4</sub>	CoC <sub>52</sub> H <sub>60</sub> N <sub>4</sub> O <sub>4</sub>	CoC <sub>52</sub> H <sub>60</sub> N <sub>4</sub> O <sub>4</sub>
Formula weight	863.97	863.97	863.97	863.97
Temperature (K)	30(2)	30(2)	30(2)	70(2)
Wavelength (Å)	0.4859	0.4859	0.4859	0.407
Crystal system	Monoclinic	Monoclinic	Monoclinic	Monoclinic
Space group	P2 <sub>1</sub> /c	P2 <sub>1</sub> /c	P2 <sub>1</sub> /c	P2 <sub>1</sub> /c
Unit cell dimensions (Å, °)	$a = 15.0105(4)$ $b = 22.2654(5)$ $c = 7.25855(15)$ $\beta = 95.027(2)$	$a = 15.0289(2)$ $b = 22.2988(4)$ $c = 7.25697(11)$ $\beta = 94.9922(15)$	$a = 15.0289(2)$ $b = 22.2988(4)$ $c = 7.25697(11)$ $\beta = 94.9922(15)$	$a = 14.9502(4)$ $b = 22.1189(4)$ $c = 7.27080(14)$ $\beta = 97.159(2)$
Volume (Å <sup>3</sup> )	2416.58(10)	2422.78(7)	2422.78(7)	2385.59(9)
Z	2	2	2	2
Density calc. (Mg/m <sup>3</sup> )	1.187	1.184	1.184	1.203
$\mu$ (mm <sup>-1</sup> )	0.402	0.401	0.401	0.407
F(000)	918	918	918	918
Crystal size (mm <sup>3</sup> )	0.1 x 0.15 x 0.2	0.1 x 0.15 x 0.2	0.1 x 0.15 x 0.2	0.1 x 0.15 x 0.2
$\Delta\theta$ for data collection (°)	1.964 to 17.678	1.860 to 17.676	1.860 to 17.678	1.877 to 17.677
Index ranges	-16 ≤ h ≤ 13, -27 ≤ k ≤ 27, -9 ≤ l ≤ 9	-2 ≤ h ≤ 18, -25 ≤ k ≤ 24, -5 ≤ l ≤ 8	-18 ≤ h ≤ 18, -27 ≤ k ≤ 27, -9 ≤ l ≤ 9	-18 ≤ h ≤ 18, -27 ≤ k ≤ 27, -9 ≤ l ≤ 9
Reflections collected	6766	4661	49498	38252
Independent reflections	4486 [R(int) = 0.1232]	2940 [R(int) = 0.0356]	4926 [R(int) = 0.0537]	4829 [R(int) = 0.0437]
Completeness to $\theta = 17.677^\circ$ (%)	82.0	59.4	99.5	99.2
Refinement method	Full-matrix least-squares on $F^2$	Full-matrix least-squares on $F^2$	Full-matrix least-squares on $F^2$	Full-matrix least-squares on $F^2$
Data / restraints / parameters	4047 / 36 / 271	2940 / 36 / 271	4926 / 36 / 271	4829 / 36 / 271
Goodness-of-fit on $F^2$	0.953	1.250	1.085	1.051
Final R indices [I > 2 $\sigma$ (I)]	R1 = 0.0333, wR2 = 0.0848	R1 = 0.0428, wR2 = 0.1092	R1 = 0.0386, wR2 = 0.1011	R1 = 0.0443, wR2 = 0.1154
R indices (all data)	R1 = 0.0374, wR2 = 0.0875	R1 = 0.0486, wR2 = 0.1124	R1 = 0.0403, wR2 = 0.1024	R1 = 0.0505, wR2 = 0.1204
Largest diff. peak and hole (e.Å <sup>-3</sup> )	0.347 and -0.305	0.297 and -0.200	0.674 and -0.492	0.709 d -0.404

\* Partial data integration. CIF file was not deposited in CCDC.

Table S6. Crystal data, measurement and refinement data for representative attenuated hard X-rays (AHAX) experiments.

Measurement Code	AHAX6 (RUN 2)*	AHAX6	AHAX3	AHAX1
Empirical formula	CoC <sub>52</sub> H <sub>60</sub> N <sub>4</sub> O <sub>4</sub>	CoC <sub>52</sub> H <sub>60</sub> N <sub>4</sub> O <sub>4</sub>	CoC <sub>52</sub> H <sub>60</sub> N <sub>4</sub> O <sub>4</sub>	CoC <sub>52</sub> H <sub>60</sub> N <sub>4</sub> O <sub>4</sub>
Formula weight	431.98	431.98	431.98	431.98
Temperature (K)	30(2)	30(2)	75(2)	110(2)
Wavelength (Å)	0.4859	0.4859	0.4859	0.4859
Crystal system	Monoclinic	Monoclinic	Monoclinic	Monoclinic
Space group	P2 <sub>1</sub> /c	P2 <sub>1</sub> /c	P2 <sub>1</sub> /c	P2 <sub>1</sub> /c
Unit cell dimensions (Å, °)	<i>a</i> = 14.9984(9) <i>b</i> = 22.2988(8) <i>c</i> = 7.2744(3) $\beta$ = 96.245(5)	<i>a</i> = 14.9984(9) <i>b</i> = 22.2988(8) <i>c</i> = 7.2744(3) $\beta$ = 96.245(5)	<i>a</i> = 14.9997(8) <i>b</i> = 22.1680(7) <i>c</i> = 7.3046(3) $\beta$ = 97.299(4)	<i>a</i> = 15.2237(13) <i>b</i> = 22.4657(13) <i>c</i> = 7.4024(4) $\beta$ = 97.330(6)
Volume (Å <sup>3</sup> )	2418.5(2)	2418.5(2)	2409.19(18)	2511.0(3)
Z	4	4	4	4
Density calc. (Mg/m <sup>3</sup> )	1.186	1.186	1.191	1.143
$\mu$ (mm <sup>-1</sup> )	0.401	0.401	0.403	0.387
F(000)	918	918	918	918
Approximated Crystal size (mm <sup>3</sup> )	0.1 x 0.15 x 0.2	0.1 x 0.15 x 0.2	0.1 x 0.15 x 0.2	0.1 x 0.15 x 0.2
$\Delta\theta$ for data collection (°)	2.140 to 17.676	1.868 to 17.676	1.872 to 17.678	1.844 to 17.678
Index ranges	-18 $\leq h \leq$ 18, -27 $\leq k \leq$ 22, -9 $\leq l \leq$ 9	-18 $\leq h \leq$ 18, -27 $\leq k \leq$ 27, -9 $\leq l \leq$ 9	-18 $\leq h \leq$ 18, -27 $\leq k \leq$ 27, -9 $\leq l \leq$ 9	-19 $\leq h \leq$ 18, -28 $\leq k \leq$ 28, -9 $\leq l \leq$ 9
Reflections collected	9312	23874	23901	15406
Independent reflections	4127 [R(int) = 0.0678]	4816 [R(int) = 0.0771]	4817 [R(int) = 0.0733]	4797 [R(int) = 0.2046]
Completeness to $\theta = 17.677^\circ$ (%)	83.7	97.7	97.7	96.8
Refinement method	Full-matrix least-squares on F <sup>2</sup>	Full-matrix least-squares on F <sup>2</sup>	Full-matrix least-squares on F <sup>2</sup>	Full-matrix least-squares on F <sup>2</sup>
Data / restraints / parameters	4127 / 36 / 271	4816 / 36 / 271	4817 / 36 / 271	4972 / 36 / 271
Goodness-of-fit on F <sup>2</sup>	1.075	1.040	1.079	1.013
Final R indices [I $\geq 2\sigma$ (I)]	R1 = 0.0722, wR2 = 0.1817	R1 = 0.0693, wR2 = 0.1666	R1 = 0.0676, wR2 = 0.1690	R1 = 0.0740, wR2 = 0.1542
R indices (all data)	R1 = 0.1110, wR2 = 0.1987	R1 = 0.0965, wR2 = 0.1807	R1 = 0.0963, wR2 = 0.1843	R1 = 0.1350, wR2 = 0.1794
Largest diff. peak and hole (e Å <sup>-3</sup> )	1.579 and -0.484	1.931 and -0.617	1.745 and -0.548	1.334 and -0.434

\*\* Partial data integration. CIF file was not deposited in CCDC.

## Selected interatomic distances

Intermolecular hydrogen bonds are labeled C<sub>ar</sub>-H $\cdots$ O<sub>diox</sub> and C<sub>ar</sub>-H $\cdots$ N<sub>ciano</sub> where C<sub>ar</sub>, N<sub>ciano</sub> and O<sub>diox</sub> are carbon atoms of the pyridine ring, nitrogen from the cyano group and the oxygen atoms of the dioxolene group respectively.

Table S7. Selected interatomic distances of representative hard X-rays (HAX) measurements.

HAX interatomic distances (Å)				
Bond type	Atoms	30 K	50 K	70K
Co-L	Co-O1	2.0160(9)	1.9535(13)	1.9032(12)
	Co-O2	2.0066(10)	1.9390(14)	1.8995(13)
	Co-N1	2.1222(12)	2.0400(16)	1.9753(16)
Intramoleclar C <sub>ar</sub> -H $\cdots$ O <sub>diox</sub>	C15-H15 $\cdots$ O1	2.9701(19)	2.896(3)	2.840(2)

	C19-H19 <sup>iii</sup> O1 <sup>i</sup>	3.0449(19)	2.947(3)	2.880(2)
Intermolecular C <sub>ar</sub> -H <sup>iii</sup> O <sub>diox</sub>	C16-H16 <sup>ii</sup> O2 <sup>ii</sup>	3.1939(18)	3.180(2)	3.204(2)
Intermolecular C <sub>ar</sub> -H <sup>iii</sup> N <sub>ciano</sub>	C18-H18 <sup>iii</sup> N2 <sup>iii</sup>	3.395(2)	3.405(3)	3.428(3)

$$i = -x, 1-y, 1-z; ii = x, y, 1+z, iii = x, -y+1/2, z-1/2$$

Table S8. Selected interatomic distances of representative attenuated hard X-rays (AHAX) measurements.

AHAX interatomic distances (Å)				
Bond type	Atoms	30 K	75 K	110 K
Co-L	Co-O1	1.965(2)	1.896(2)	1.916(2)
	Co-O2	1.952(2)	1.896(2)	1.923(2)
	Co-N1	2.057(3)	1.971(3)	1.998(3)
Intramolecular C <sub>ar</sub> -H <sup>iii</sup> O <sub>diox</sub>	C15-H15 <sup>iii</sup> O1	2.917(4)	2.843(4)	2.871(5)
	C19-H19 <sup>iii</sup> O1 <sup>i</sup>	2.969(4)	2.872(4)	2.909(5)
Intermolecular C <sub>ar</sub> -H <sup>iii</sup> O <sub>diox</sub>	C16-H16 <sup>ii</sup> O2 <sup>ii</sup>	3.205(4)	3.223(4)	3.275(5)
Intermolecular C <sub>ar</sub> -H <sup>iii</sup> N <sub>ciano</sub>	C18-H18 <sup>iii</sup> N2 <sup>iii</sup>	3.407(5)	3.430(4)	3.485(6)

$$i = -x, 1-y, 1-z; ii = x, y, 1+z, iii = x, -y+1/2, z-1/2$$

The interatomic distances obtained for **1** from the X-ray diffraction data provided two values for Co–O and one value for Co–N distances in each temperature. Similarly to the procedure used by Ribeiro *et al.*<sup>7</sup>, using the refined Co–L distances for a given temperature ( $D_{exp}^{Co-L}$ ), we could compute the  $hs-[Co^{+2}(SQ^*)_2]$  isomer mole fraction for a given distance,  $(\gamma(hs-Co^{2+})_L)$ , by the following equation:

$$\gamma(hs-Co^{2+})_L = (D_{exp}^{Co-L} - D_{Co^{3+}}^{Co-L}) / (D_{Co^{2+}}^{Co-L} - D_{Co^{3+}}^{Co-L}), \quad (1)$$

L stands for O and N atoms,  $D_{Co^{3+}}^{Co-L}$  and  $D_{Co^{2+}}^{Co-L}$  are the values of Co–L distances in  $ls-[Co^{+3}(SQ^*)(Cat^2)]$  and  $hs-[Co^{+2}(SQ^*)_2]$  reference states respectively, averaged from distances surveyed in CCDC<sup>6</sup>:

$$\begin{aligned} D_{Co^{3+}}^{Co-N} &= 1.940(16) \text{ Å} & D_{Co^{2+}}^{Co-N} &= 2.151(7) \text{ Å} \\ D_{Co^{3+}}^{Co-O1} &= 1.889(6) \text{ Å} & D_{Co^{2+}}^{Co-O1} &= 2.060(5) \text{ Å} \\ D_{Co^{3+}}^{Co-O2} &= 1.872(12) \text{ Å} & D_{Co^{2+}}^{Co-O2} &= 2.045(2) \text{ Å} \end{aligned}$$

The average  $\gamma(hs-Co^{2+})$  value for a given temperature was obtained by averaging the values obtained for each Co ion neighbor with equation (2):

$$\gamma(hs-Co^{2+}) = \frac{1}{3} \sum_L \gamma(hs-Co^{2+})_L \quad L = O, N. \quad (2)$$

The values for  $\gamma(hs-Co^{2+})$  with the corresponding standard deviations were used in Figures 3 and 4 of the manuscript.

## Molecule superposition

Figure S1 shows the molecular geometry of **1** and its superposition and packing at different temperatures.

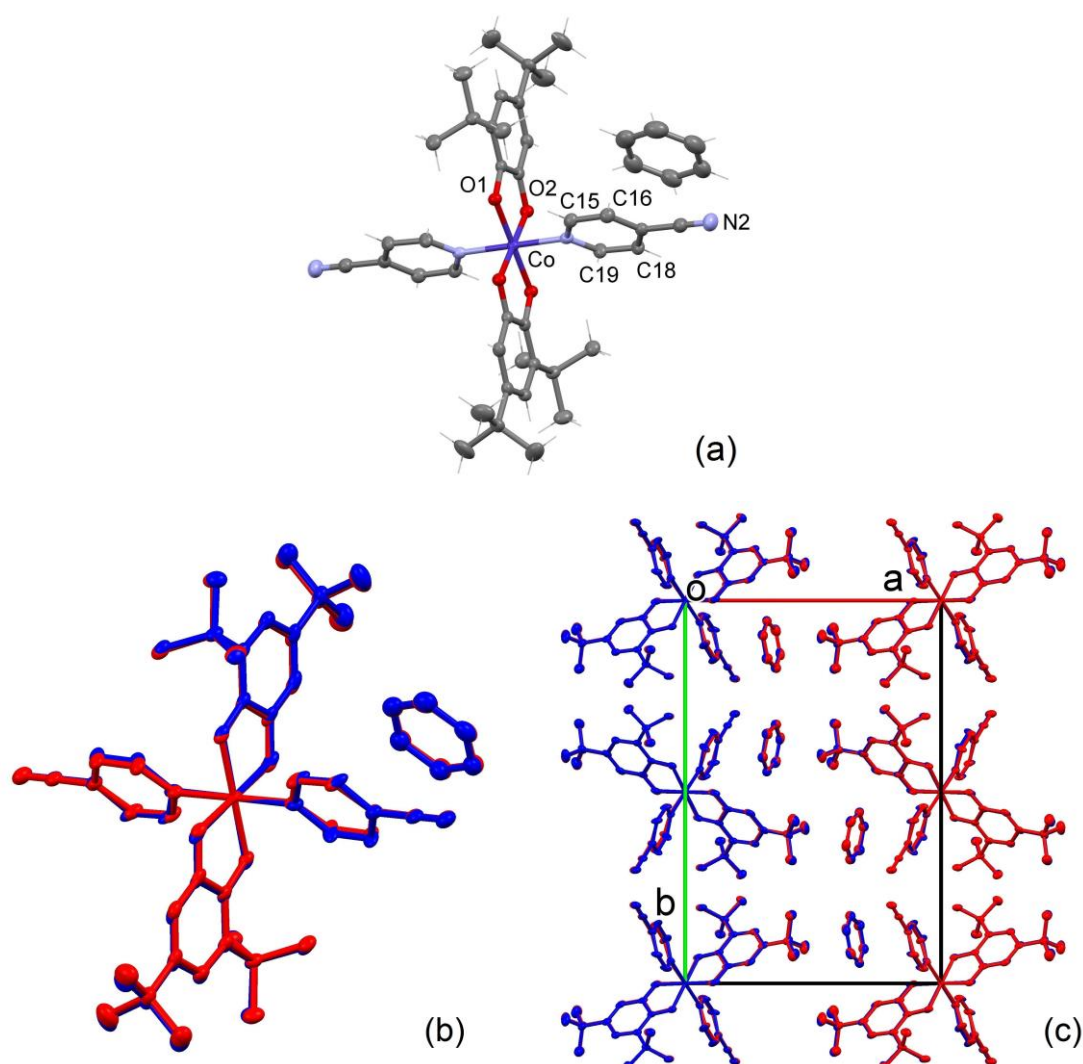


Figure S1. Molecular geometry (a), superposition (b) and packing (c) of **1** at 30 K (blue) and 60 K (red) from Hard X-rays (HAX) experiments. Ellipsoids are drawn at the 50% of probability level.

## References

- (1) Nowell, H.; Barnett, S. A.; Christensen, K. E.; Teat, S. J.; Allan, D. R. I19, the Small-Molecule Single-Crystal Diffraction Beamline at Diamond Light Source. *J. Synchrotron Radiat.* **2012**, 19 (3), 435–441.
- (2) CrysAlisPro. *Rigaku Oxford Diffraction, CrysAlisPro Software System*; CrysAlisPro suite; Rigaku Corporation, Oxford, UK, 2015.
- (3) Altomare, A.; Cascarano, G.; Giacovazzo, C.; Guagliardi, A.; Burla, M. C.; Polidori, G.; Camalli, M. SIR92 – a Program for Automatic Solution of Crystal Structures by Direct Methods. *J. Appl. Crystallogr.* **1994**, 27 (3), 435–435.
- (4) Sheldrick, G. M. SHELXT – Integrated Space-Group and Crystal-Structure Determination. *Acta Crystallogr. Sect. Found. Adv.* **2015**, 71 (1), 3–8.
- (5) Johnson, C. K. Introduction to Thermal- Motion Analysis. In *Crystallographic Computing Proceedings of an international Summer School*; Ahmed, F. R., Hall, S. R., Huber, C. P., Eds.; Munksgaard, Copenhagen: Ottawa, 1970; pp 207–219.
- (6) Allen, F. H. The Cambridge Structural Database: A Quarter of a Million Crystal Structures and Rising. *Acta Crystallogr. B* **2002**, 58 (3), 380–388.

- (7) Ribeiro, M. A.; Stasiw, D. E.; Pattison, P.; Raithby, P. R.; Shultz, D. A.; Pinheiro, C. B. Toward Controlling the Solid State Valence Tautomeric Interconversion Character by Solvation. *Cryst. Growth Des.* **2016**.